

Laminar–turbulent transition in Poiseuille pipe flow subjected to periodic perturbation emanating from the wall.

Part 2. Late stage of transition

By G. HAN, A. TUMIN AND I. WYGNANSKI†

Faculty of Engineering, Tel-Aviv University, Tel-Aviv 69978, Israel

(Received 25 May 1999 and in revised form 7 March 2000)

Transition in a fully developed circular pipe flow was investigated experimentally by introducing periodic perturbations. The simultaneous excitation of helical modes having indices $m = \pm 1, \pm 2$ and ± 3 was chosen. The experiments revealed that the late stage of transition is accompanied by the formation of streaky structures that are associated with peaks and valleys in the azimuthal distribution of the streamwise velocity disturbance. The breakdown to turbulence starts with the appearance of spikes in the temporal traces of the velocity. Spectral characteristics of these spikes and the direction of their propagation relative to the wall are similar to those in boundary layers. Analysis of the data suggests the existence of a high-shear layer in the instantaneous velocity profile.

Additional experiments in which a very weak, steady flow was added locally to the periodic axisymmetric perturbation were also carried out. These experiments resulted in the generation of a single peak in the azimuthal distribution of the disturbance amplitude. The characteristics of the transition process (spikes, vortical patterns etc.) within this peak were similar to ones observed in the helical excitation experiments. Based on these results one may conclude that late stages of transition in a pipe flow and in a boundary layer are similar. The present report is part of an ongoing investigation that was initiated by Eliahou, Tumin & Wygnanski (1998*a*).

1. Introduction

This paper describes an experimental investigation of a late stage of transition in a circular pipe flow subjected to periodic perturbations emanating from the wall. The investigation is a continuation of the experiments initiated by Eliahou, Tumin & Wygnanski (1998*b*, hereafter referred to as ETW).

Transition from laminar to turbulent flow in a circular pipe is often referred to as ‘bypass transition’ (see Morkovin & Reshotko 1990; Morkovin 1993; Reshotko 1994). The parabolic velocity profile is linearly stable and the transition scenario has to bypass the stage of Tollmien–Schlichting (TS) waves existing in boundary layer flows.

Leite (1959) introduced axially symmetric disturbances of large amplitude into a fully developed flow and revealed that transition to turbulent flow takes place

† Also at the Department of Aerospace and Mechanical Engineering, The University of Arizona, Tucson, Arizona 85721, USA.

whenever the disturbance amplitude exceeds a certain threshold level that decreases with increasing Reynolds number. Fox, Lessen & Bhat (1968) excited their pipe flow with two helical modes having indices $m = \pm 1$. They concluded that their disturbances could be unstable and established a ‘neutral curve’ in the ‘frequency–Reynolds number’ plane. Rubin, Wygnanski & Haritonidis (1980) introduced a pulsed disturbance into a fully developed Poiseuille flow and concluded that the resulting transitional flow was similar to the flow disturbed at the inlet. Darbyshire & Mullin (1995) extended the previous experiments with disturbances introduced into fully developed pipe flow. They established that a critical amplitude of the disturbance was required to cause transition, and showed its dependence on Reynolds number. Recent experiments by Draad, Kuiken & Nieuwstadt (1998) revealed that the critical amplitude also depends on the disturbance frequency. Their qualitative results, requiring a threshold amplitude to cause transition, are in agreement with numerical simulations describing the onset of turbulence in pipe flows (Boberg & Brosa 1988).

ETW investigated a bypass transition in a circular pipe flow with help of controlled disturbances. The disturbances were generated by eight acoustic drivers that provided periodic blowing and suction through eight slots in the wall. Most of the experiments were carried out by simultaneous generation of two opposing helical modes $m = \pm 2$. The results of ETW indicated that transition to turbulence occurs when streamwise vortices develop due to a nonlinear interaction of helical modes, distorting the time-averaged velocity profile. To clarify the role of the streamwise vortices, they were also generated artificially by four weak steady jets that were superposed on the small-amplitude, periodic, helical disturbances. The experiment revealed that there is a self-sustaining mechanism, when the weak streamwise rolls support the instability of the helical modes of indices $m = \pm 2$ which, in turn, amplify the steady vortices.

The periodicity in the azimuthal direction of the streamwise vortices observed by ETW is reminiscent of the spanwise periodicity of streamwise vortices in the experiments by Klebanoff, Tidstrom & Sargent (1962). One can suggest that there might be a considerable similarity between the respective transition mechanisms in boundary layers and in pipes. Hot-wire measurements by Eliahou *et al.* (1998a) revealed that the transition process is accompanied by the appearance of spikes in the velocity history and the amplitude spectra of these spikes were similar to those observed by Borodulin & Kachanov (1995). These observations provided the motivation for the present work, that endeavours to describe the details of the late stages of transition in a pipe flow and to compare them with observations made in a boundary layer. Hereafter, the term ‘late stage of transition’ implies the stage when spikes appear in the temporal traces of the velocity.

We shall recapitulate briefly what is known about the late stages of transition in boundary layers (more detailed information may be found in the reviews by Kachanov 1994 and by Bowles 2000). Hama, Long & Hegarty (1957) visualized the flow in a disturbed boundary layer in a water tank and observed the formation of a Λ -vortex in the transition zone. Klebanoff *et al.* (1962) discovered the existence of streamwise vortices in the flow field near the surface, by measuring two velocity components. To emulate the ‘natural’ spanwise modulation of the flow and to control its spanwise variation they placed strips of tape beneath the vibrating ribbon. The interaction between stationary disturbances and travelling waves led to strong spanwise modulation of the flow. (Weak steady jets were used by ETW to obtain azimuthal variation in the flow near the surface of a pipe.) The maxima in the spanwise distribution of the streamwise-periodic velocity disturbance were called ‘peaks’, the minima ‘valleys’. The breakdown to turbulence was observed at the ‘peak’ locations and was

accompanied by strong negative fluctuations in the streamwise velocity component, commonly referred to as *spikes*. The number of spikes could double and triple with increasing downstream distance. Kovaszny, Komoda & Vasudeva (1962) measured three velocity components that were phase locked to the oscillations of the ribbon and concluded that a very intense vortex layer is periodically formed in the boundary layer. The high-shear layer had a shape of a delta wing in a plan view that was inclined to the surface in the elevation view. The sharp negative pulse in the oscilloscope trace (a spike) was associated with a ‘kink’ in the vortex sheet that was deduced from the data representing the vorticity distribution in the elevation view. Detailed flow-field visualization made by Hama & Nutant (1963) reinforced the notion that Λ -shaped vortex loops exist. They observed that a primary Λ -vortex creates a strong upward fluid motion in between its legs, thus forming a high-shear layer. Subsequently, small Ω -shaped vortex (observed by Klebanoff *et al.* (1962), and called a hairpin vortex) was observed to separate from the apex of the Λ -vortex. Williams, Fasel & Hama (1984), who measured the three velocity components, confirmed the concept of the vortex loop. Vorticity in the loop is mainly oriented in the downstream direction, while the vorticity in the high-shear layer is predominantly in the spanwise direction. The magnitude of the spanwise vorticity component in the high-shear layer is three times larger than in the loop and it is also two times larger than the maximum vorticity in the undisturbed laminar boundary layer. Experiments by Kachanov *et al.* (1984, 1985, 1989), and Borodulin & Kachanov (1988) revealed that the spikes have a deterministic periodic structure that arises from amplification of the higher harmonics. A detailed study of the spike properties was carried out in Borodulin & Kachanov (1988).

The main features of laminar–turbulent transition are usually attributed to Klebanoff and are referred to as the K-regime of breakdown. The K-regime is recognized by the alignment of the Λ -vortices in rows. Kachanov, Kozlov & Levchenko (1977) discovered that transition might be accompanied by a staggered array of Λ -vortices and referred to it as the N-regime. A detailed discussion of the physical mechanisms associated with the K- and N-regimes is given by Kachanov (1994). The alternative name for the transition accompanied by a staggered array of Λ -vortices is the H-regime (after Herbert, who developed a theoretical model for this type of transition). We keep here the terminology introduced by Kachanov (1994) for the latter regime (N-regime). Bake, Kachanov & Fernholz (1996) showed that the alignment of the coherent structures during the late stages of transition can assume either N- or K-modes without changing the nature of the breakdown process. The formation of the Λ -patterns in the K- and N-regimes is different, but both lead to the formation of high-shear layers and spikes during the late stage of the transition process.

The late stage of transition was also investigated by direct numerical simulations (DNS, for a review see Kleiser & Zang 1991). Rist & Fasel (1995) carried out a spatial DNS of a transitional boundary layer and confirmed the main experimental observations described by Williams *et al.* (1984). Rist & Fasel (1995) made a detailed comparison of their experimental data with DNS results. The agreement between physical and numerical experiments showed that DNS is a very powerful tool for analysing fine structures in the transition zone. In particular, DNS proved that the spikes are associated with ring-like (or Ω -like) vortices that separate from the tips of the large Λ -vortices.

The above describes the conventional thinking that evolved following the seminal paper by Klebanoff *et al.* (1962). For a comprehensive recapitulation we have to discuss a scenario of *oblique transition*. Schmid & Henningson (1992) considered

transition initiated by a pair of oblique modes (O-regime) in a channel flow by using a temporal DNS. Joslin, Street & Chang (1992) and Berlin, Lundbladh & Henningson (1994) investigated the oblique transition scenario with spatial DNS in boundary layers. Due to nonlinear interaction, the pair of oblique waves gives rise to streamwise vortices, which in turn lead to low- and high-speed streaks of large amplitude due to the lift-up effect. The breakdown to turbulence results from the secondary instability of the streaks (Reddy *et al.* 1998). Experiments concerned with the oblique transition were carried out by Elofsson & Alfredsson (1998) in plane Poiseuille flow and by Elofsson (1998) and Berlin, Wiegel & Henningson (1999) in boundary layers. The experiments support the DNS results concerning the breakdown to turbulence through the secondary instability of the streaks. The recent numerical and experimental investigation by Berlin *et al.* (1999) discovered that Λ -patterns also appear during the late stage of oblique transition. Thus, there is a similarity between flow structures at the late stage of transition in K-, N- and O-regimes.

One can recognize that experiments by ETW and those presented in this paper deal with an oblique type of transition because they start with two opposing helical modes. However, one should keep in mind that the term ‘oblique transition’ is usually used in conjunction with the supposition that the streamwise vortices evolve from a linear mechanism consistent with the theories of *non-modal growth*.

Ellingsen & Palm (1975) considered the inviscid case of an initial disturbance that is independent of the streamwise coordinate and found that the streamwise-disturbance amplitude may grow in time, even though the basic flow does not possess an inflection point. Landahl (1980) showed that all parallel inviscid shear flows are unstable to a wide class of three-dimensional disturbances. The result is independent of whether the shear flow is unstable or not to exponential growth of wave-like disturbances. This type of instability, that is not related to an exponential growth, is referred to as ‘non-modal growth’.

Hultgren & Gustavsson (1981) considered the temporal evolution of a three-dimensional disturbance in a boundary layer and found that the initial growth is followed by a viscous decay (transient growth). The investigations by Gustavsson (1991), Butler & Farrell (1992), Reddy & Henningson (1993), and Trefethen *et al.* (1993) showed a great potential for bypass transition resulting from the non-modal growth. The phenomenon of transient growth was studied in pipe flow numerically by Boberg & Brosa (1988), O’Sullivan & Breuer (1994) and Ma *et al.* (1999). Theoretical analysis of transient growth in pipe Poiseuille flow within the scope of temporal theory was carried out by Bergström (1992, 1993), Schmid & Henningson (1994), and Trefethen, Trefethen & Schmid (1999). Mayer & Reshotko (1997) performed an analysis of transient growth in a circular pipe, and concluded that the phenomenon had been observed experimentally by Kaskel (1961). We should point out that the theoretical analysis of transient growth was carried out within the framework of a temporal theory, while a spatial development is observed in experiments. Recently, Reshotko & Tumin (1999) generalized the method of Schmid & Henningson (1994) for spatial disturbances of a prescribed frequency. The calculations revealed that stationary disturbances may achieve a more significant transient growth than non-stationary ones. The maximum transient growth exists at azimuthal index $m = 1$ for stationary perturbations, whereas non-stationary perturbations may achieve their maxima at higher azimuthal indices. The spatial analysis confirmed the potential of the non-modal growth for bypass transition.

Morkovin (1993) distinguished ‘strong-disturbance bypasses – category *S*’ and ‘weak-disturbance bypasses – category *W*’. A bypass of category *S* may be observed

in a high-disturbance environment, while a W -bypass may manifest itself in a lower-disturbance environment. The oblique transition scenario comprising the non-modal linear growth mechanism is an example of the W -bypass. Ma *et al.* (1999) performed numerical simulations of a pipe flow subjected to periodic blowing and suction at small and finite amplitudes. The results demonstrated the transient growth mechanism and a possibility of the oblique transition scenario.

Although the experiments by ETW deal with the oblique type of transition, they revealed that there is a self-sustaining mechanism responsible for high-amplitude streaks. The observation is consistent with theoretical models by Waleffe (1997) and Bergström (1999). It is conceivable that the amplitudes chosen in the experiment were too high and the linear non-modal growth could not be observed behind the stronger self-sustained amplification. We do not pursue a discussion of possible mechanisms responsible for formation of high-amplitude streaks since the topic of our research is the late stage of transition. (We refer to the paper by Baggett & Trefethen 1997 where they suggest that the different models might be much closer than it appears at first glance.)

Reuter & Rempfer (1998) modelled numerically the experiments of ETW and found that the transition process is accompanied by Λ -like (hairpin-like) vortices. This result together with observations of spikes (Eliahou *et al.* 1998a) indicates that there is a similarity between the late stages of the transition processes in a boundary layer (K-, N- and O-types) and in a circular pipe flow.

The object of the present paper is to reinforce experimentally the notion of similarity between the late stages of transition in both of these flows, and perhaps expand this notion to other wall-bounded flows.

2. Apparatus and instrumentation

The experiments were carried out in a 33 mm diameter (D) and 17 m long aluminium pipe (described in detail by ETW). The new feature of the system is an advanced version of the disturbance generator. The disturbances were generated by eight acoustic drivers (as it was done in ETW) but the perturbations were now conveyed to 24 settling chambers located around the pipe (instead of eight chambers used by ETW). Another difference is that the mixing among the jets originating from adjacent chambers occurred inside a common chamber that lead to a slot. The idea was proposed by Gaponenko & Kachanov (1994) for their boundary-layer experiments. The common chamber serves to smooth interactions between neighbouring jets. A further improvement was associated with the exit from the common chamber to the pipe. To avoid a local separation near the exit, it was inclined at 45° to the flow direction. Although the width of the exit slot was adjustable, the experiments were carried out at constant 2.8 mm width in the direction of streaming. A photograph illustrating a part of the disturbance generator is shown in figure 1. To observe the evolution of the disturbance at various distances from the generator, a few interchangeable pipe sections were affixed to the generator, which was located at $X/D = 400$ from the pipe inlet.

Measurements were done using a constant-temperature hot-wire anemometer manufactured by AA Lab Systems Ltd. The hot-wire element itself was made of tungsten, $5\ \mu\text{m}$ in diameter and about 1 mm in length. Two types of hot-wire probes were used in the experiments. The first one was a single standard DANTEC P14 probe. The probe was used for measurements of streamwise velocity at any specific location (r, θ, x) . The second one was a hot-wire array of seven parallel wires for simultaneous

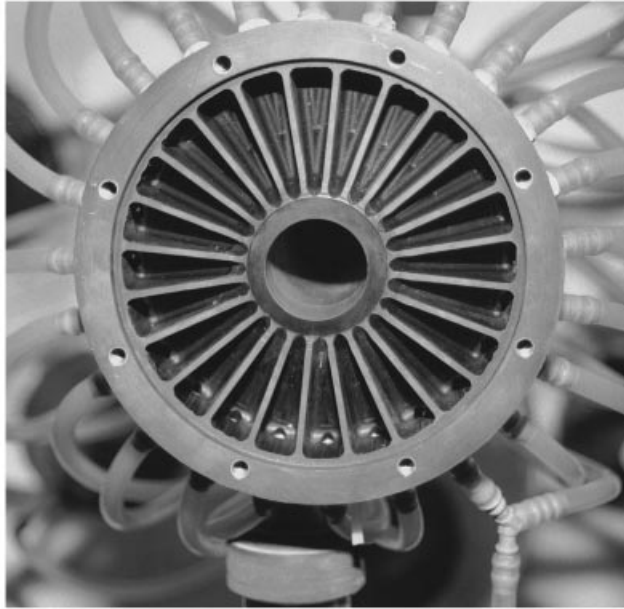


FIGURE 1. Open disturbance generator with 24 settling chambers.

measurement of the streamwise velocity and its radial derivative. The radial length of the array was equal to 3.3 mm. A special traversing mechanism was designed to move the hot-wire array around under computer control. Initial alignment of the probes was accomplished as described by ETW, i.e. by blocking the pipe exit with a plug containing small holes 0.2 mm in diameter. The probes were calibrated against the local dynamic pressure monitored by a Validyne DP-103 pressure transducer. The variation of the anemometer voltage output with velocity was approximated by a third-order polynomial. The calibration was carried out between 0.2 m s^{-1} and 3 m s^{-1} . The data from the hot-wire probes, sampled at a frequency of 950 Hz each, together with a reference signal, were digitized and stored on a PC. The disturbance signal was used for phase reference.

Signals for the disturbance source were generated by a computer interface board made by the National Instruments Corporation. The ten independent 12-bit voltage output channels of this board were used as a source for the prescribed signal generation. The output signal was amplified by a ten-channel power amplifier, built at Tel-Aviv University for activating the loudspeakers. The resulting pressure perturbation of the same amplitude was distributed to three settling chambers chosen among 24 chambers available in order to get the best output for the required azimuthal mode. In preparation for the present experiments, all results reported by ETW were reproduced because they helped to validate the new instrumentation.

3. Results

The disturbance frequency used in the present experiments was identical to the one used by ETW (i.e. $f = 18.5 \text{ Hz}$), and the Reynolds number was slightly higher (i.e. $Re = 2350$ instead of 2280). The amplitude of the disturbance corresponded to the so called high-amplitude regime defined by ETW, which is characterized by the

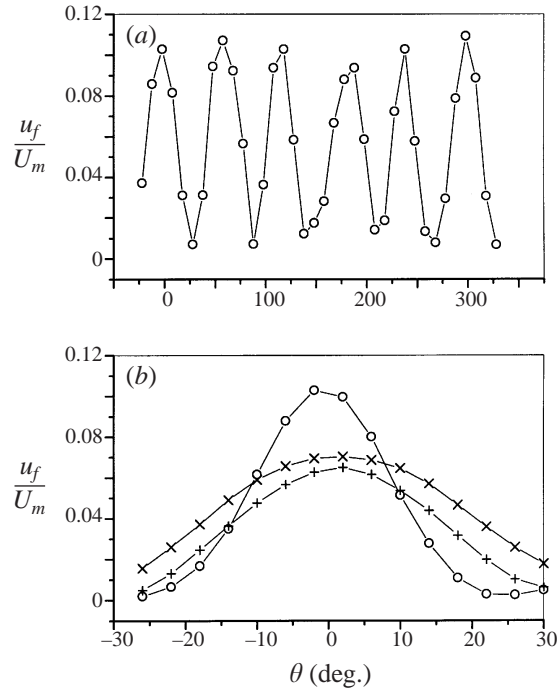


FIGURE 2. Azimuthal variation of the fundamental disturbance amplitude u_f at $r/a = 0.36$. \circ , $X/D = 1.52$; $+$, $X/D = 2.42$; \times , $X/D = 2.88$. $m = \pm 3$.

appearance of streamwise vortices and transition to turbulence. The main part of the experiments was also carried out in a similar manner with combinations of counter-rotating helical modes having indices $m = \pm 1$, $m = \pm 2$ and $m = \pm 3$. The simultaneous excitation by counter-rotating, (\pm), modes ensured the generation of steady streamwise vortices that are of great importance to the transition mechanism. Because the goal of the investigation was to concentrate on the late stage of transition, we have dealt with relatively high initial amplitudes. Keeping in mind the experimental observations by ETW that a self-sustained amplification of disturbances was generated in the pipe, we will avoid discussing the streamwise growth of the vortices as a consequence of a linear mechanism consistent with the theories of non-normal growth. We also carried out an experiment (similar to the one carried out by Borodulin & Kachanov (1995)) without the imposed periodicity in the azimuthal coordinate and we shall refer to it as to a single-peak experiment (see § 3.2).

3.1. Experiments with counter-rotating helical modes

3.1.1. Time averaged velocity

Simultaneous excitation of $\pm m$ helical modes gives rise to steady streamwise vortices of index $2m$ resulting from a nonlinear interaction. The counter-rotating streamwise rolls ensure an azimuthal redistribution of the momentum due to the lifting of fluid between adjacent pairs. The redistribution in the time-averaged velocity is accompanied by an azimuthal variation in the streamwise, periodic-in-time, disturbances that possess both peaks and valleys. The azimuthal distribution of the streamwise velocity component of the filtered disturbance amplitude (the first harmonic u_f) for $m = \pm 3$ excitation at $r/a = 0.36$ (a being the pipe radius) is shown in figure 2 (U_m

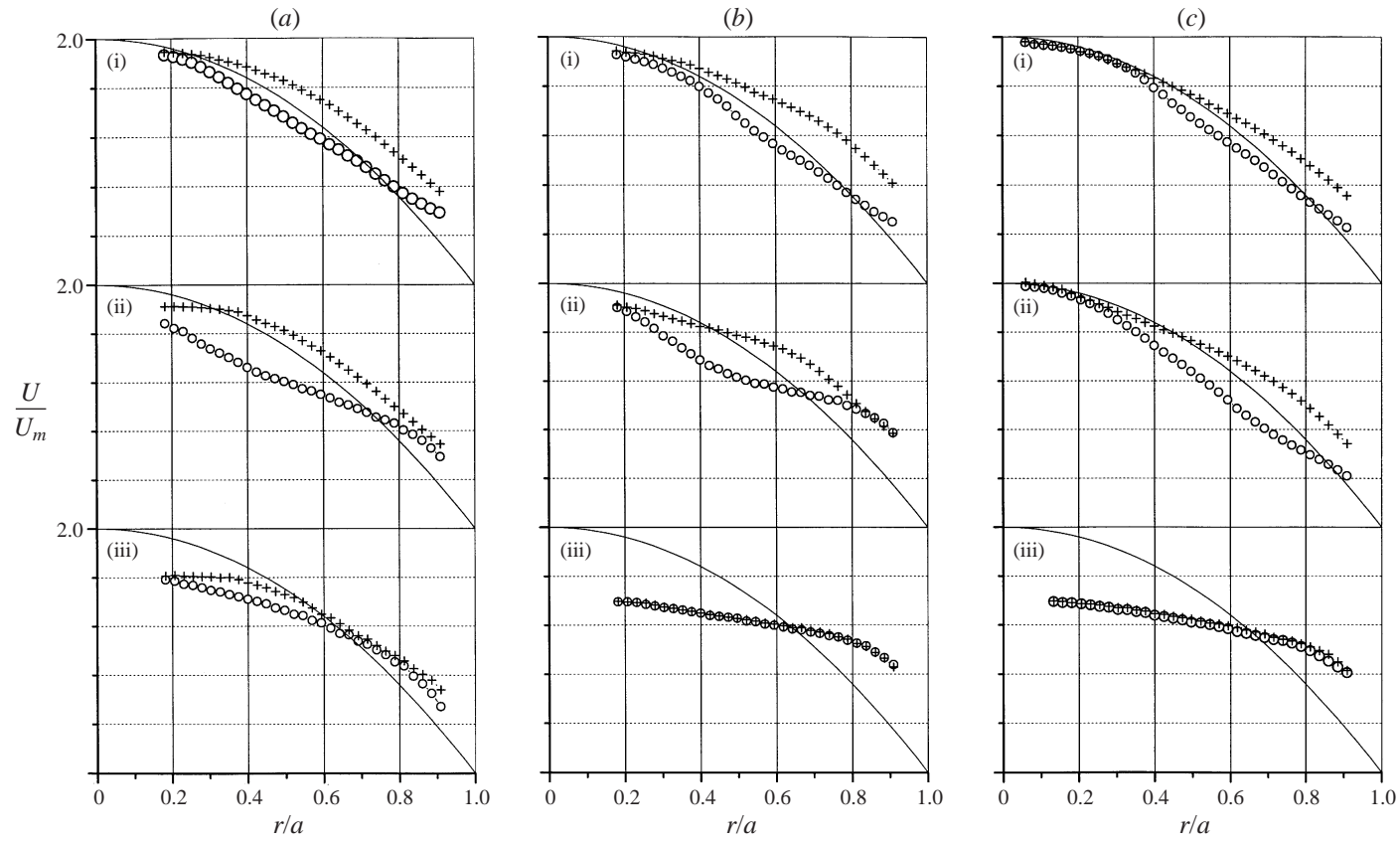


FIGURE 3. Time-averaged velocity profiles. \circ , peak; $+$, valley. (a) $m = \pm 1$, (i) $X/D = 1.52$; (ii) 3.33; (iii) 9.39. (b) $m = \pm 2$, (i) $X/D = 1.52$; (ii) 3.94; (iii) 9.39. (c) $m = \pm 3$, (i) $X/D = 1.82$; (ii) 4.70; (iii) 11.52.

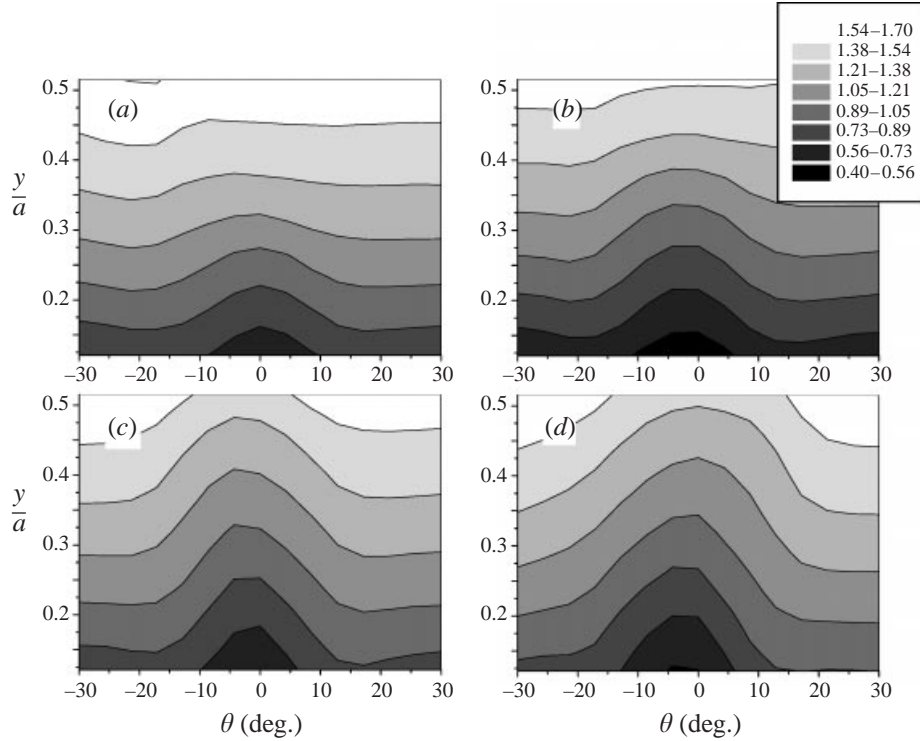


FIGURE 4. A low-speed streak in the time-averaged velocity profile U/U_m . Excitation of the helical modes $m = \pm 3$. (a) $X/D = 0.91$; (b) 1.21; (c) 1.36. (d) 1.67.

is the average velocity in the pipe). It contains six peaks whose wavelength λ_θ is approximately $a\pi/3$ (i.e. about the pipe radius). The evolution of this amplitude (distributed over $\theta = \pm 30^\circ$, i.e. $2\pi/6$) in the direction of streaming is shown in figure 2(b). The amplitude initially decreases at the peak position and increases in the valleys. Further downstream the amplitude increases at all azimuthal angles, θ . The time-averaged velocity profiles at azimuthal angles corresponding to a peak and a valley of the amplitude are plotted in figure 3 for three helical modes of excitation $m = \pm 1$; $m = \pm 2$ and $m = \pm 3$. One may observe that the velocity profile at the peak has an inflection point that is similar to the one observed in a boundary layer.

The time-averaged contours of velocity for azimuthal angles $-30^\circ < \theta < 30^\circ$ at four streamwise locations in the pipe, corresponding to $m = \pm 3$ excitation, are plotted in figure 4 (y is a distance measured from the pipe wall). One can see low-speed fluid propagating toward the centre of the pipe with increasing distance from the disturbance generator. The contour plots for $m = \pm 1$ and $m = \pm 2$ are similar, they differ in the azimuthal width of the pattern only.

3.1.2. Spike observations

The temporal velocity traces across the entire pipe corresponding to the azimuthal location of a peak amplitude are shown in figure 5 for three x -locations when the flow was excited by $m = \pm 3$ modes. The radial location of the largest spike, r_s , at various streamwise stations is presented in figure 6. When helical modes $m = \pm 1$ were excited simultaneously, the streamwise distance, over which a single spike was observed, was short and it did not extend beyond $X/D = 1.5$ downstream of the disturbance

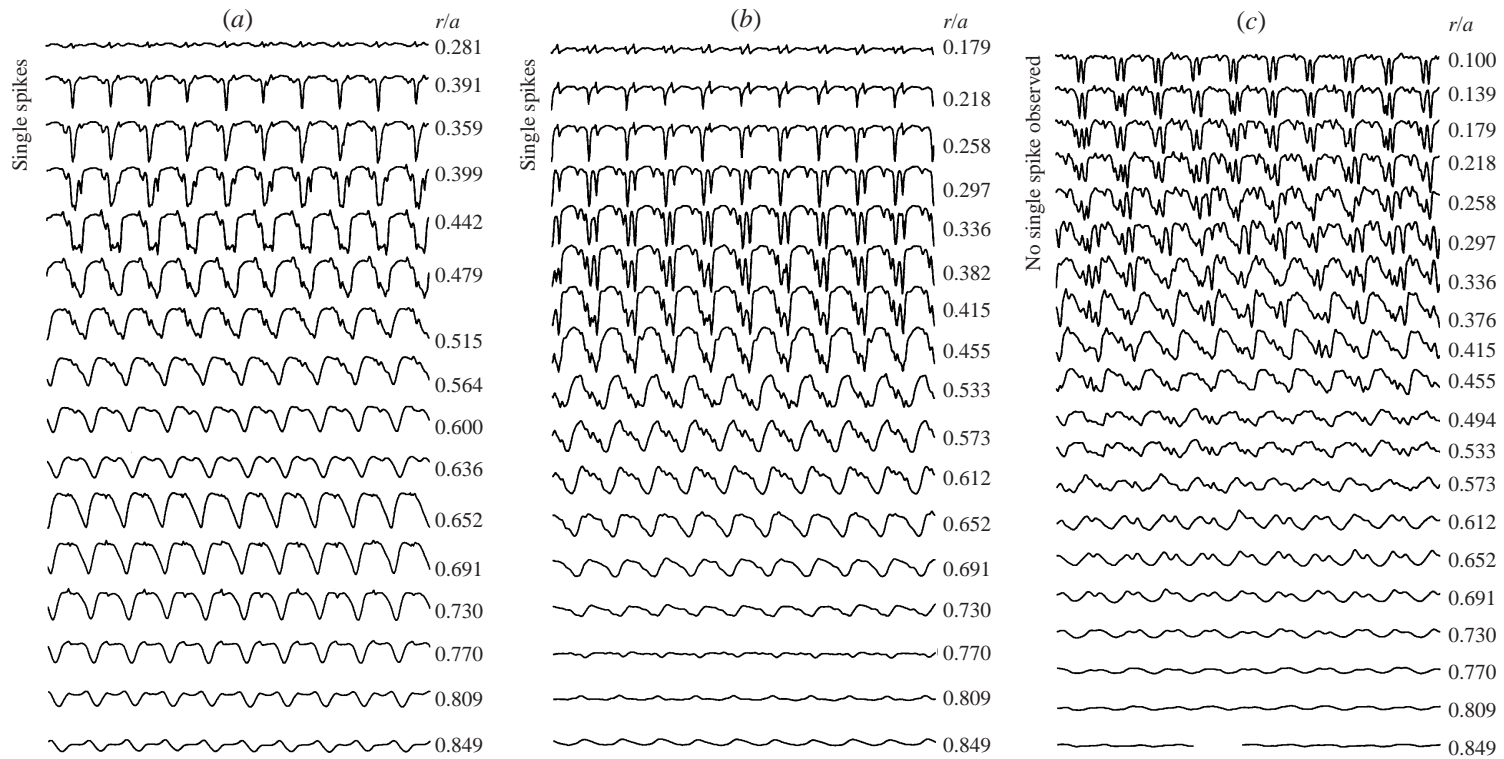


FIGURE 5. Velocity traces. Excitation of the helical modes with $m = \pm 3$. (a) $X/D = 1.67$; (b) 2.42; (c) 3.33.

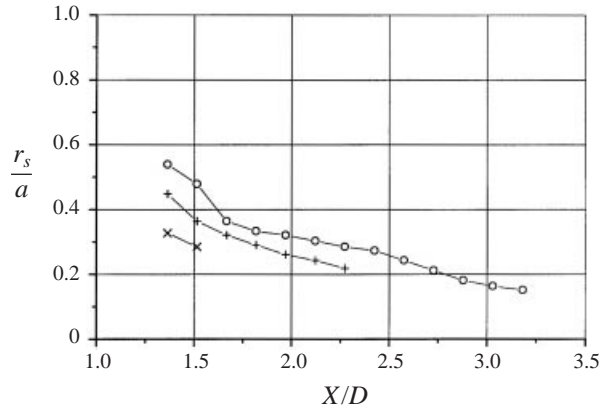


FIGURE 6. Downstream evolution of the spike coordinate determined at the maximum point of its amplitude. \times , $m = \pm 1$; $+$, $m = \pm 2$; O , $m = \pm 3$.

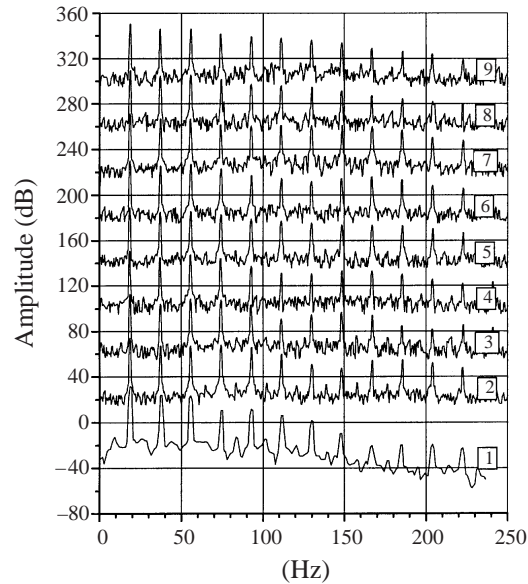


FIGURE 7. Development of disturbance-amplitude spectra obtained at spike maximum: spectra 1–9 correspond to $X/D = 1.36, 1.67, 1.97, 2.42, 2.58, 2.73, 2.88, 3.03, 3.18$ (each successive spectrum is shifted by +40 dB). Excitation of the helical modes with $m = \pm 3$.

generator. The streamwise distance over which the spike could be observed for the $m = \pm 2$ mode was longer and for the $m = \pm 3$ mode it was longer still. One can see that the spike travels toward the centre of the pipe and away from the wall as it does in boundary-layer experiments. In a boundary layer, the spike approaches the outer edge. In pipe flow, it can arrive at the pipe axis where an interaction with structures originating from different azimuthal locations takes place. In the central region, therefore, the process loses its similarity to the boundary layer, where such an interaction cannot occur. For $m = \pm 1$, where two peak regions were generated on opposite sides of the pipe ($\theta = \pm\pi$), the interaction across the radius undulates the single spikes rapidly and thus they are not seen at $X/D > 1.5$. The significance of the azimuthal interaction increases with increasing mode index m and this inhibits the

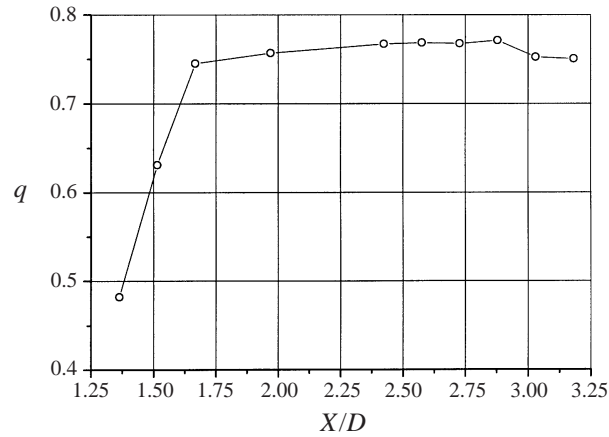


FIGURE 8. The evolution of the geometric progression factor, determined from the spectra in figure 7.

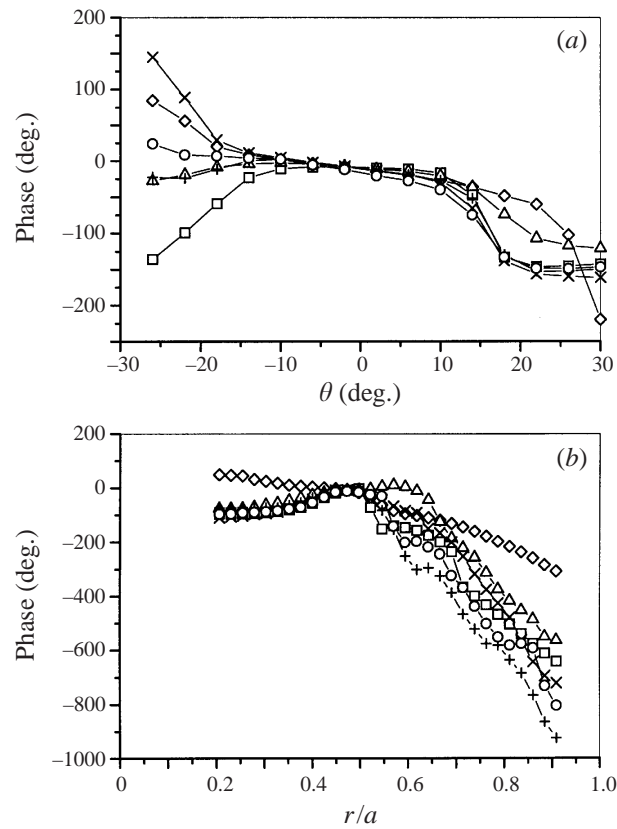
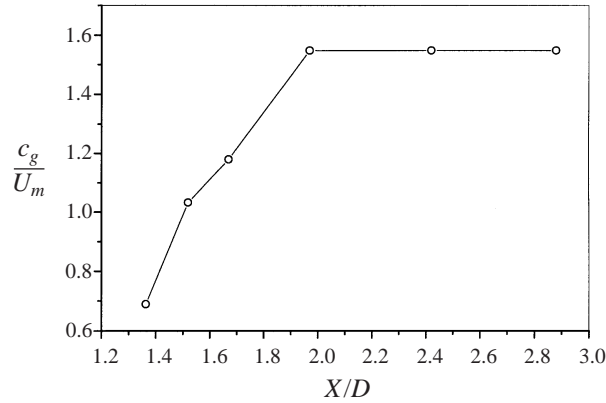


FIGURE 9. The azimuthal and radial distributions of the phases of harmonics composing the spike. $X/D = 1.52$. (a) $y/a = 0.48$; (b) $\theta = -2^\circ$. \diamond , f ; \square , $2f$; \triangle , $3f$; \times , $4f$; $+$, $5f$; \circ , $6f$. $m = \pm 3$.

radial spreading of the single spikes, making them visible for larger and larger X/D (figure 6). In the discussion that follows we shall confine our attention to the case $m = \pm 3$ while keeping the qualitative similarity to the $m = \pm 1$ and ± 2 excitations in mind.

FIGURE 10. Group velocity of the spike. $m = \pm 3$.

The amplitude spectra of the velocity disturbances corresponding to the largest spike location are shown in figure 7. The spectra were obtained from the corresponding traces that were not ensemble averaged. One can see that the spike consists of many harmonics having amplitudes A_i that decay in a geometric progression with increasing frequency. The geometric-progression factor $q = A_{i+1}/A_i$ (see figure 8) remains almost constant (about 0.75) after the formation of the single-spike structure at approximately $X/D \approx 1.7$. Figure 9 demonstrates the synchronization of the harmonic constituent of the spike for $m = \pm 3$ excitation. A comparison of the present results with experimental data obtained in the boundary layer (Borodulin & Kachanov 1988, 1995) shows that they are very similar indeed and thus the spike represents the same phenomenon in both flows.

The group velocity of the spike for the $m = \pm 3$ case is presented in figure 10. The group velocity of the single spike was calculated as $c_g = dX_s/dt$, where X_s is the spike streamwise location evaluated from the phase-locked measurements. In Borodulin & Kachanov (1995), the group velocity was approaching the velocity prevailing at the edge of the boundary layer. In our experiments it approaches the time-averaged velocity on the pipe axis. It is worth mentioning that the large bulges at the outer edge of a turbulent boundary layer propagate at $U/U_\infty \approx 0.93$ (Kovaszny, Kibens & Blackwelder 1970). The downstream evolution of phases corresponding to the leading three harmonics of the spike are shown in figure 11. The coordinates, r/a , were chosen to correspond with the peak of the disturbance. From these phase measurements we evaluated the phase velocities that are equal to $c_f/U_m = 1.36$, $c_{2f}/U_m = 1.14$ and $c_{3f}/U_m = 1.26$ for $m = \pm 2$ excitation, and they are somewhat lower for the $m = \pm 3$ excitation (i.e. $c_f/U_m = 1.04$, $c_{2f}/U_m = 1.02$ and $c_{3f}/U_m = 1.08$). In the experiments of Williams *et al.* (1984), the phase velocity of the second harmonic was within 15% of the wave speed of the fundamental disturbance inside the boundary layer. One can see that our results for the wave speeds in the $m = \pm 2$ case are similar to the results Williams *et al.* (1984). The phase velocities for the $m = \pm 3$ disturbance agree to within a few percent.

3.1.3. The high-shear layer

Kovaszny *et al.* (1962) discovered a very intense vortical layer in the transitioning boundary layer flow that had the shape of delta wing propagating downstream in the (X, Z) -plane. They deduced this by measuring instantaneous velocity profiles

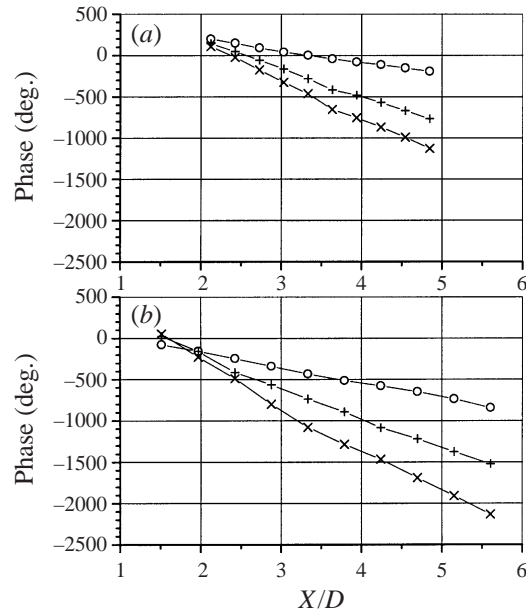


FIGURE 11. Downstream evolution of phases. (a) $m = \pm 2, r/a = 0.485$; (b) $m = \pm 3, r/a = 0.494$.
 \circ, f ; $+$, $2f$; $\times, 3f$.

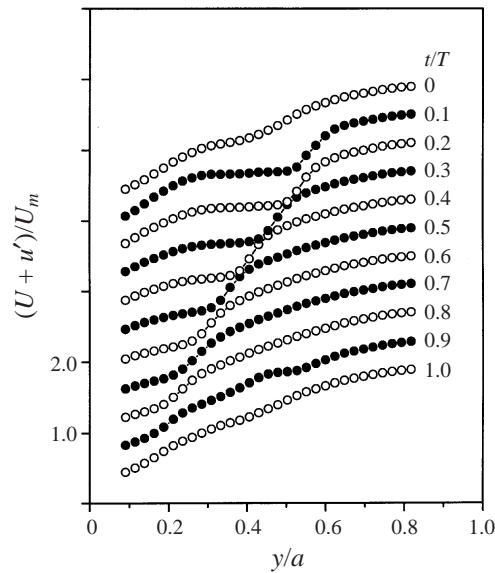


FIGURE 12. Instantaneous velocity profiles at the peak at one spike stage. $X/D = 1.52, \theta = -2^\circ$.
 $m = \pm 3$. Each successive profile is shifted by $0.4U_m$.

(using an array of hot wires) at various phases of their vibrating ribbon. The shear layer observed in the transitional pipe flow is now compared to the observations of Kovaszny *et al.* (1962). Instantaneous velocity profiles measured at different phases of the forcing cycle at a location corresponding to the dominance of a single spike (peak, $X/D = 1.52$) are plotted in figure 12. One may observe the appearance of the

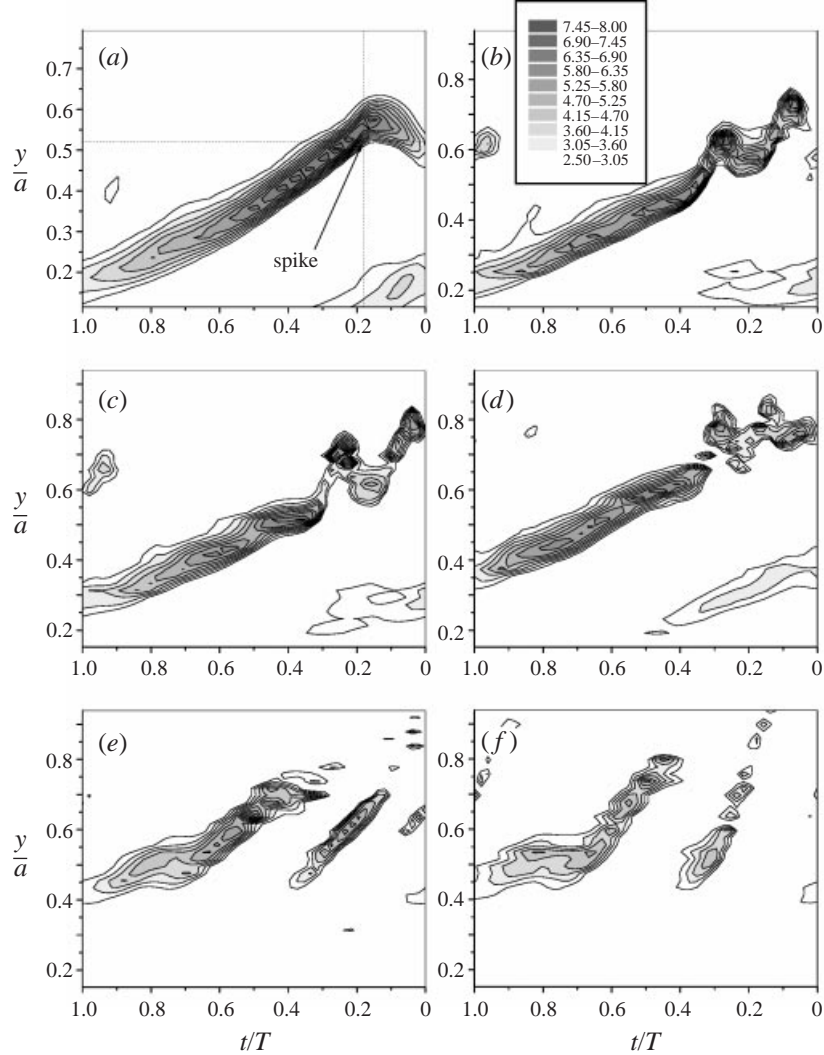


FIGURE 13. Development of the high-shear layer $a/U_m \partial(U + u')/\partial y$ at the peak in the case $m = \pm 3$. (a) $X/D = 1.52$; (b) 1.97; (c) 2.42; (d) 3.33; (e) 4.70; (f) 5.15. Ensemble averaging of 70 events.

high-shear layer at $t/T = 0.1$, at $y/a = 0.6$ and its migration toward the wall with increasing time. The instantaneous velocity gradient is about 2 times larger than the maximum gradient observed in the undisturbed pipe flow. This observation agrees with similar ones made in boundary layers.

Dimensionless contours of $\partial(U + u')/\partial y$, which represents the main component of the azimuthal vorticity (at the azimuthal location corresponding to the peak), are shown in figure 13 for increasing X/D . At $X/D = 1.52$ the shear layer has a typical shape that was observed in the boundary layer during the one-spike stage. The leading edge is bent down (toward the wall) and a ‘kink’ appears in the vortex pattern. This ‘kink’ is associated with a spike. At $X/D = 1.97$ a second ‘kink’ developed and a second spike was observed in the temporal velocity traces. Further downstream ($X/D > 4$) the breakdown of the shear layer becomes apparent.

The plan view of the shear layer measured at $X/D = 1.52$ (each point corresponds

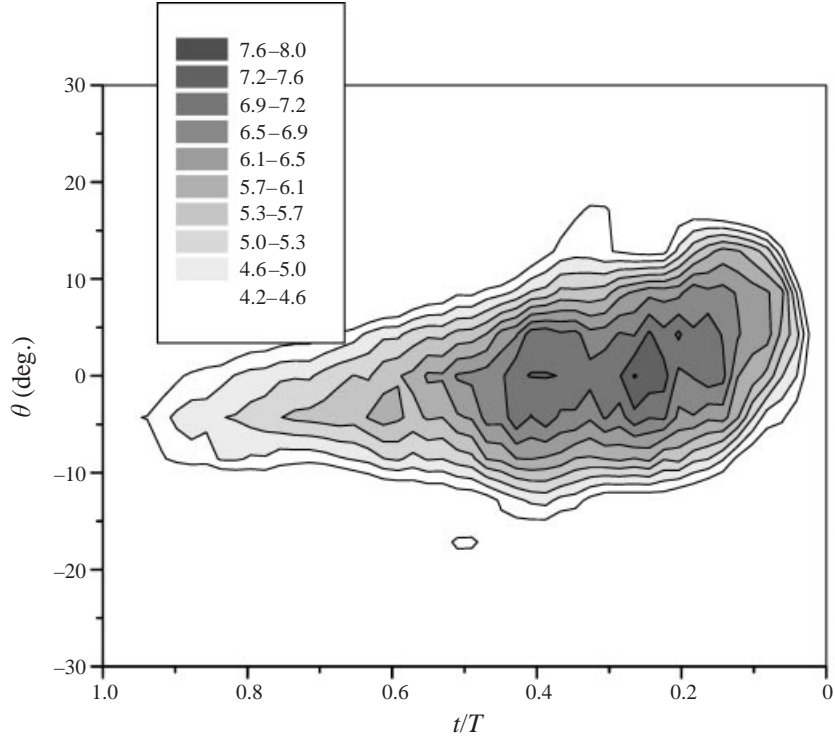


FIGURE 14. High-shear layer $a/U_m \partial(U + u')/\partial y$ for the $m = \pm 3$ case. $X/D = 1.52$. Ensemble averaging of 70 events.

to y/a of its local maximum value) is shown in figure 14. Contrary to the delta-wing shape observed in a plane boundary layer (Kovasznay *et al.* 1962) the present azimuthal vorticity contours resemble a 'tadpole', the difference being attributed to the difference in the flow geometry. In the experiments of Kovasznay *et al.* (1962) the base of the shear-layer pattern (measured near the surface) was about five boundary-layer thicknesses wide. The characteristic scale in the pipe flow, corresponding to the boundary-layer thickness, is the pipe radius, and there is insufficient azimuthal distance to attain a similarity with the pattern generated in the boundary layer.

Two shear layers, one measured at the peak and the other in the valley, together with the corresponding instantaneous velocity profiles are plotted in figure 15 and they may be compared with figure 16 of Williams *et al.* (1984). The time in this figure (seen by a stationary observer located at $X/D = 1.52$) increases from right to left. The foot of the velocity profile gives its corresponding time value. The patterns are similar to the observations made by Williams *et al.* (1984).

The understanding of the mechanism responsible for the formation of the high-shear layer during the transition process is a task addressed by experimentalists and computers alike. It was recognized (see §1) that a Λ -vortex is generated in the flow. The streamwise vorticity in the vortex legs creates a strong upward fluid motion in the interior of the Λ thus forming a high-shear layer. The existence of a vortex loop near the head of the Λ -vortex was demonstrated both numerically and experimentally (Rist & Fasel 1995; Rist & Kachanov 1994). The vortex loop is associated with the appearance of a spike in the temporal velocity traces. To reconstruct the complete vorticity field, one has to carry out measurements of all

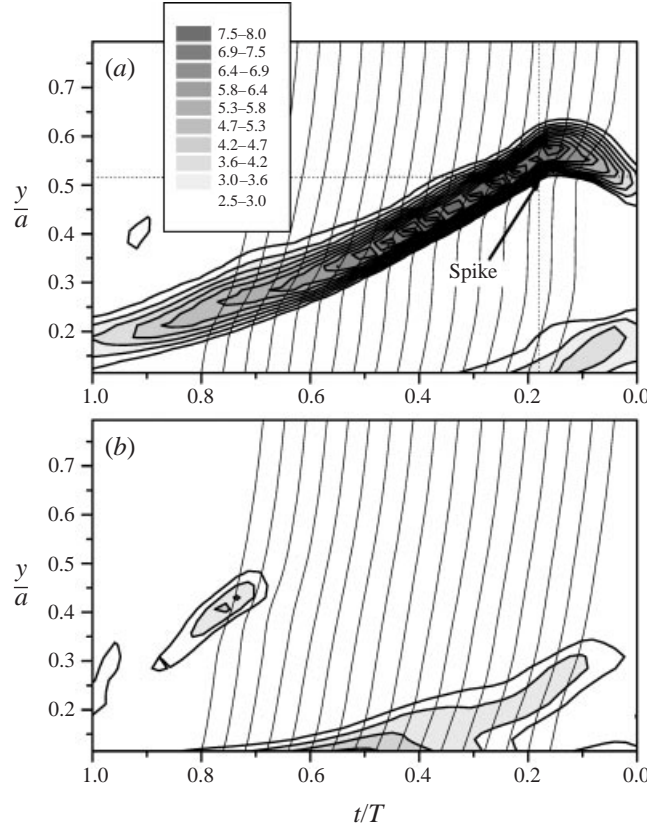


FIGURE 15. Contours of the high-shear layer $a/U_m \partial(U + u')/\partial y$ with the instantaneous velocity profiles in the (y, t) -plane at $X/D = 1.52$. (a) peak; (b) valley. Ensemble averaging of 70 events.

three velocity components. Borodulin *et al.* (1998) suggested illustrating the pattern at a given cross-section by considering the total, instantaneous velocity gradient $[(\partial(U + u')/\partial y)^2 + (\partial(U + u')/\partial z)^2]^{1/2}$ in the (y, z) -plane. The shape was reminiscent of an Ω . When the same idea was applied to pipe-flow experiments, the instantaneous velocity gradient was calculated as $[(\partial(U + u')/\partial r)^2 + r^{-2}(\partial(U + u')/\partial \theta)^2]^{1/2}$ (figure 16). One can see that the pattern is not as well shaped as the Ω observed in a boundary layer because of possible interactions from opposite sides of the pipe.

We can speculate that there is a vorticity loop having legs that are almost aligned with the direction of streaming that resembles a hairpin vortex with its legs aligned with the pipe axis.

3.2. A single-peak experiment

An isolated spanwise non-uniformity was generated in the amplitude of the fundamental instability wave by Borodulin & Kachanov (1995). This was done by glueing two strips of adhesive tape under the oscillating ribbon that provided the primary disturbance. Thus, a solitary peak was observed along the span, in the amplitude distribution of the streamwise component of velocity. Generating an isolated peak in the pipe flow is also helpful because it provides more space for development of the vortices prior to their inevitable interaction with other participants in the process. We provided a local non-uniformity in the flow by adding a weak steady jet that

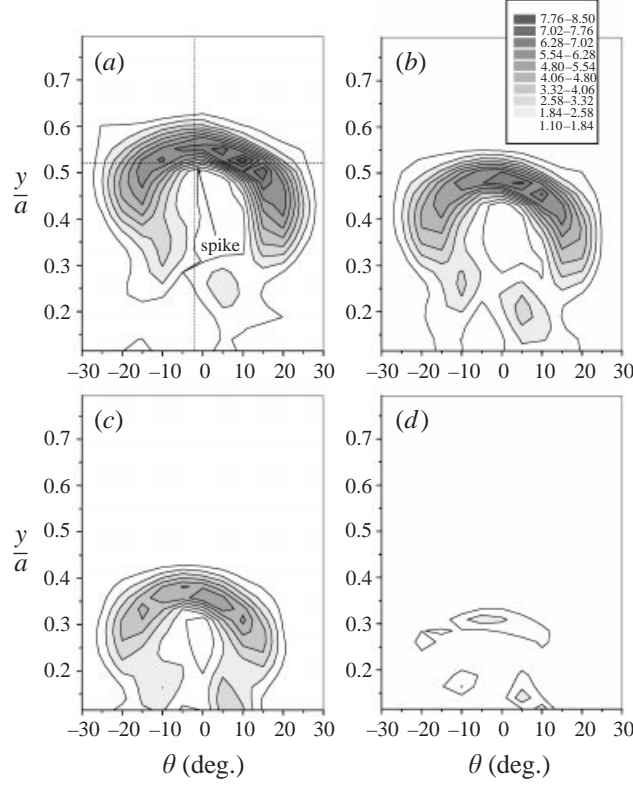


FIGURE 16. The instantaneous velocity gradient in the (y, θ) -plane at $X/D = 1.52$. (a) $t/T = 0.18$; (b) -0.29 ; (c) -0.49 ; (d) -0.69 . Ensemble averaging of 70 events.

exhausted through a slot. The two-dimensional fundamental disturbance used in the boundary layer was replaced by an axisymmetric disturbance ($m = 0$) in the pipe. Whereas the experiments using helical modes of indices $\pm m$ are similar to the experiments concerned with oblique type of transition in boundary layers, the single-peak experiment resembles the introduction of a large-amplitude TS-wave in a flat-plate boundary layer. As it was discovered by Berlin *et al.* (1999), the late stages of oblique transition are all alike in boundary layers, and one may expect that the same will hold in the pipe.

3.2.1. Time-averaged velocity

The time-averaged velocity contours in the (y, θ) -plane are shown in figure 17. The low-speed streak in the time-averaged velocity profile corresponds to the peak in azimuthal distribution of the disturbance amplitude. The azimuthal variation of the amplitude of the fundamental harmonic at $r/a = 0.39$ corresponding to the maximum amplitude at $\theta = 0$ is shown in figure 18. It is obvious that the azimuthal widths of the streaks and their disturbance amplitude variation have approximately the same values as in the experiments that used simultaneous excitation of $m = \pm 3$ modes (figure 2b). As a consequence, we expect that the results for the single-peak experiment would be similar to the results discussed in § 3.1.

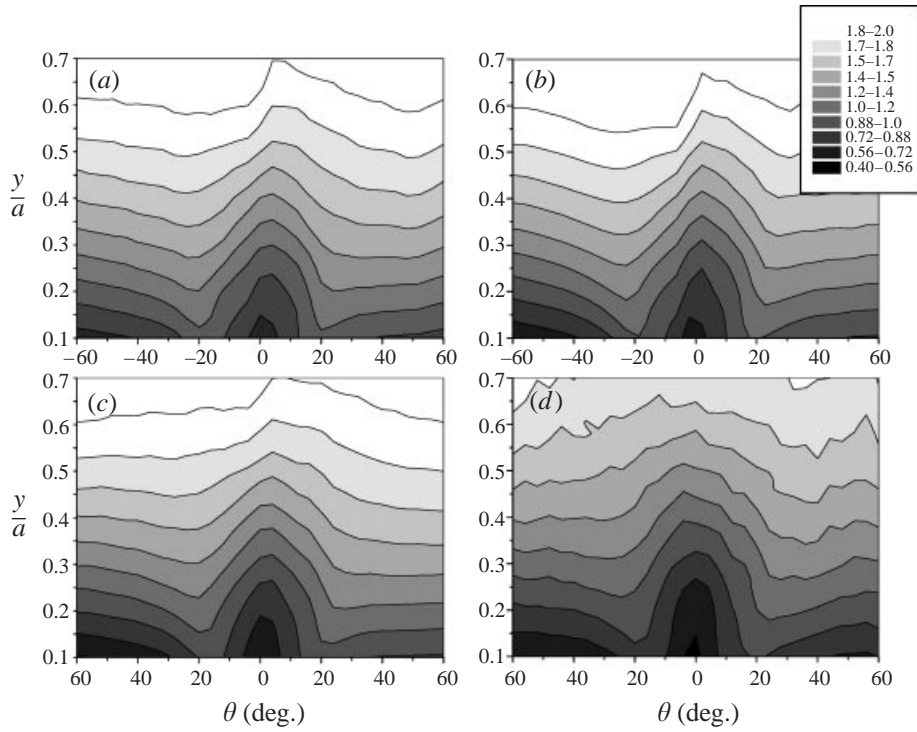


FIGURE 17. A low-speed streak in the time-averaged velocity profile. The single-peak experiment. (a) $X/D = 1.21$; (b) 1.36; (c) 1.52. (d) 1.82. Ensemble averaging of 70 events.

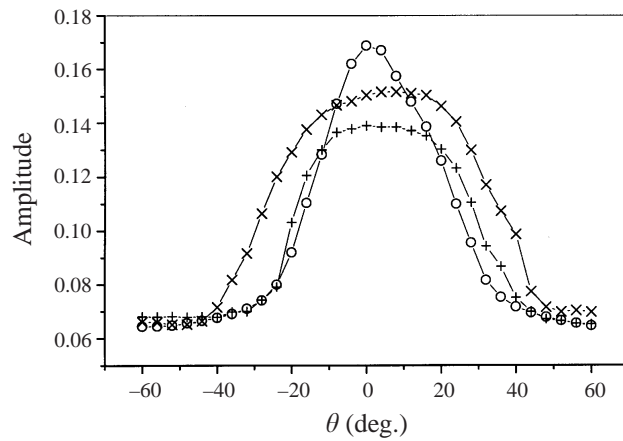


FIGURE 18. Azimuthal variation of the fundamental disturbance amplitude u_f at $r/a = 0.39$. \circ , $X/D = 1.52$; $+$, $X/D = 2.42$; \times , $X/D = 2.88$.

3.2.2. Spike observations

The time histories of the streamwise velocity component are similar to those observed in §3.1.2 (figure 5) where one could recognize the formation and the development of spikes. Once again the radial location of the spike approaches the pipe axis with increasing distance from the disturbance generator (figure 19). The

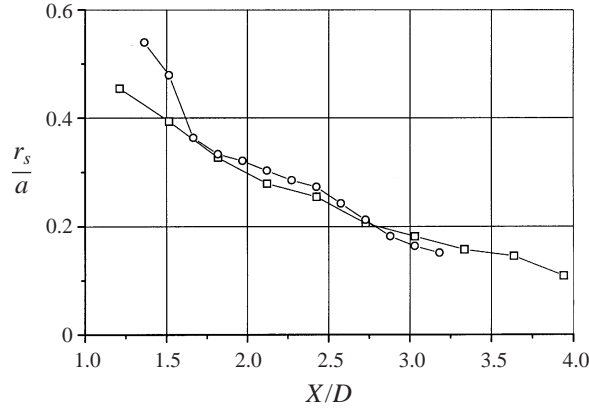


FIGURE 19. Downstream evolution of the spike coordinate determined at the maximum point of its amplitude: \square , single-peak experiment; \circ , helical modes ± 3 .

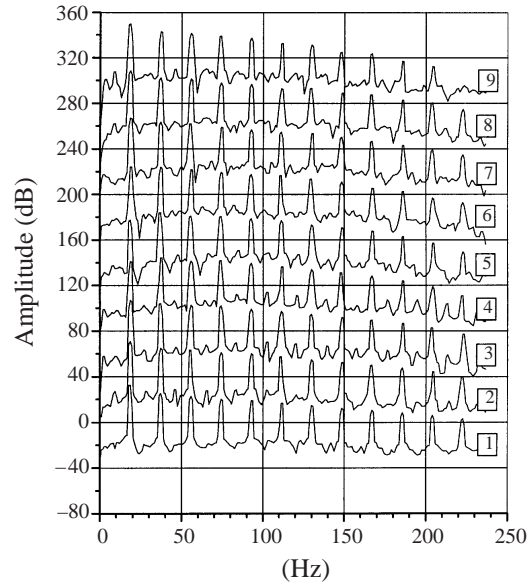


FIGURE 20. Development of disturbance amplitude spectra obtained at spike maximum: spectra 1–9 correspond to $X/D = 1.52, 1.82, 2.12, 2.42, 2.73, 3.03, 3.33, 3.64, 3.94$ (each successive spectrum is shifted by +40 dB). The single-peak experiment.

spectra of the disturbance, at a location corresponding to the spike maximum also reveal the presence of many higher harmonics with amplitudes that diminish in a geometric progression (figure 20). The geometric progression factor remains almost constant (about 0.75) as it was in the experiments with counter-rotating helical modes. One may observe (figure 20) the appearance of a subharmonic $f_{1/2} = f/2$ and various sums of frequencies like $3f/2, 5f/2, \dots$ (e.g. see spectrum 2) in figure 20. This may be attributed to subharmonic resonance interactions between the strong axisymmetric (forced) wave and the undisturbed helical modes existing in the background.

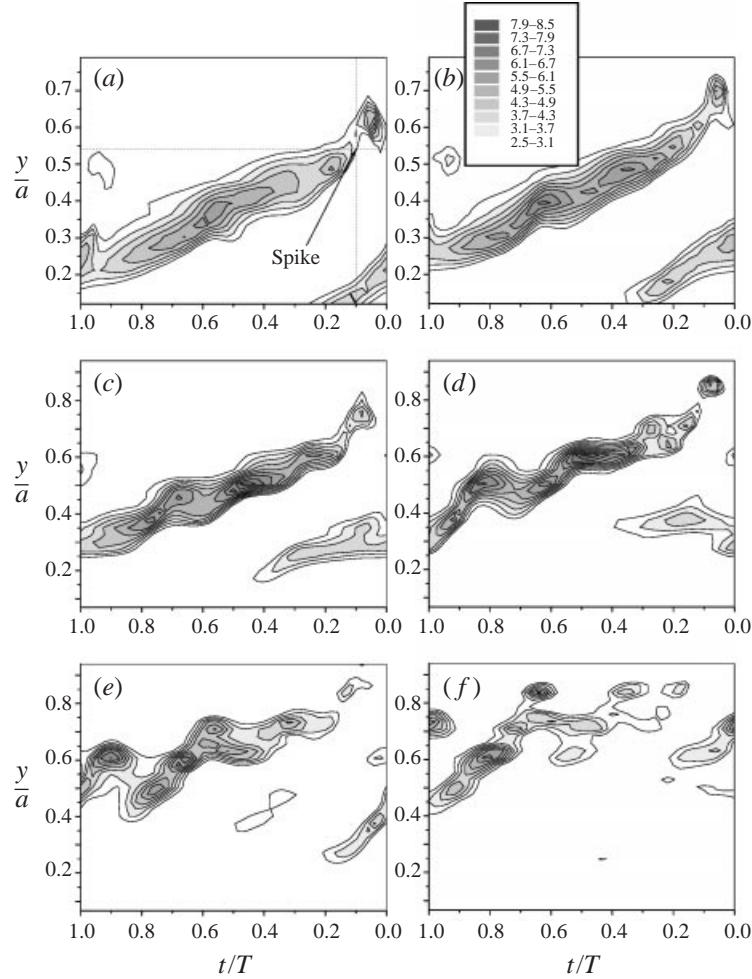


FIGURE 21. Development of the high-shear layer $a/U_m \partial(U + u')/\partial y$ in the single-peak experiment. (a) $X/D = 1.21$; (b) 1.52; (c) 1.82; (d) 2.42; (e) 3.03; (f) 3.94. Ensemble averaging of 70 events.

3.2.3. The high-shear layer

The results obtained in a single-peak experiment carried out in transitional pipe flow are now discussed. The development and breakdown of the high-shear layer that is characterized by $(a/U_m)\partial(U + u')/\partial y$ with increasing distance from the disturbance generator is shown in figure 21.

One can see that many of the features discussed in §3.1.3 (such as the formation of a ‘kink’ that is associated with the appearance of a spike in the temporal traces of velocity, the inclination of the shear layer to the surface and its eventual disintegration) are reproduced in this experiment. Specific details in the development of the high-shear layer may differ due to differences in initial amplitudes, time-averaged velocity field etc., but the same physical mechanisms appear to control the route to transition. One may note, for example, the regular wavy appearance of the vorticity contours seen in figure 21(c–e) that were not seen in figure 13. This might be the result of random helical buffet rather than the orderly azimuthal periodicity. The width of the high-shear layer in plan view is almost constant (figure 22). The instantaneous

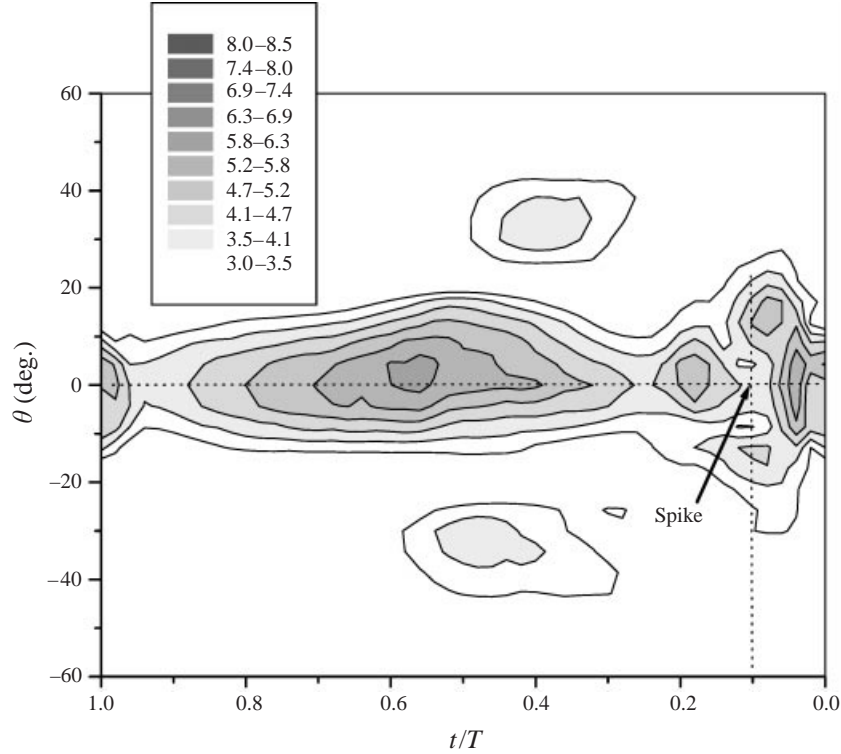


FIGURE 22. High-shear layer $a/U_m \partial(U + u')/\partial y$ at $X/D = 1.21$ in the single-peak experiment. Ensemble averaging of 70 events.

velocity gradient in the (y, θ) -plane is shown in figure 23. There is a well-shaped Ω -pattern. Once again, this shape agrees with observations made in a boundary layer (Borodulin *et al.* 1998). Although the shape of the high-shear layer in the plan view is different from the delta-wing shape observed in boundary layer flows, the structure at $t/T = 0.0 - 0.2$ is the same. The results also indicate that there is a vorticity loop whose legs are approximately aligned with the direction of streaming, and it looks like a typical hairpin vortex.

4. Discussion and summary of the results

The experiments of ETW indicated that transition to turbulence in a fully developed pipe flow can occur only after the parabolic profile was distorted by longitudinal vortices. Such a distortion may be generated by a steady or by a periodic disturbance. The vortices may be amplified due to the linear mechanism of non-modal growth, or due to a self-sustaining mechanism. In the present experiment the specific features of the late stages of laminar–turbulent transition in a pipe were explored. It follows that an ‘elementary constituent’ of the process is a hairpin vortex with its ‘head’ deflected toward the pipe axis. The hairpin vortex generates a low-speed streak between its legs as it does in a boundary layer. This results in a formation high-shear layer. When counter-rotating helical modes are excited, a system of peaks and valleys in the disturbance amplitude is formed similar to the ones observed in a boundary layer with each peak corresponding to a low-speed streak near the surface and a creation of the high-shear layer across the flow (be it in a boundary layer or in a pipe). As the

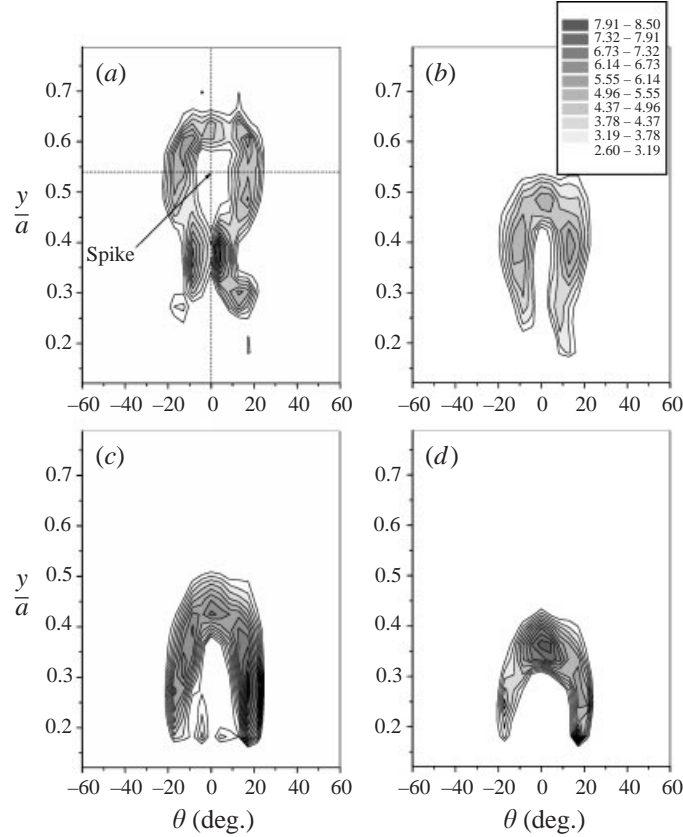


FIGURE 23. The instantaneous velocity gradient in the (y, θ) plane at $X/D = 1.21$. (a) $-t/T = 0.10$; (b) -0.12 ; (c) -0.40 ; (d) -0.60 . Ensemble averaging of 70 events.

shear layer travels downstream, a ‘kink’ appears in its elevation view (in the (r, x) -plane) just above the low-speed bump. It is manifested by a spike in the temporal records of the streamwise velocity. The main features of the spike in a pipe are again very similar to those in a boundary layer. With the passage of time the spike not only propagates downstream but it also propagates across the flow. In the boundary layer, spikes propagate toward the boundary layer edge, while in the pipe flow, spikes approach the pipe axis. In this case they may interact with spikes coming from the other areas of the pipe. Owing to this focusing, the highly deterministic picture that was observed in a boundary layer is destroyed. This may be a source for a more rapid randomization process in the pipe. Therefore, in spite of many similarities between transition in boundary layers and pipe flow that have been established in the present work, the geometry specifics might reveal some other paths to transition. The same phenomenon may also be observed in a plane Poiseuille flow where the peak–valley structures are generated simultaneously near both opposing walls.

Recently, Reuter & Rempfer (2000) accomplished a DNS simulation representing the current experiments with helical $m = \pm 3$ excitation. Their results support the experimental observations regarding spikes, high-shear layer and hairpin vortices.

The observation of a bypass transition due to the generation of hairpin vortices is not new in transition experiments. Klebanoff *et al.* (1962) had already observed

a bypass of the linear stage whenever the initial amplitude of the perturbation was large. Subcritical transition triggered by the generation of hairpin eddies was investigated experimentally in a plane Poiseuille flow and in a boundary-layer flow by Nishioka & Asai (1985), Asai & Nishioka (1995, 1997) and Asai, Sawada, & Nishioka (1996). It was pointed out that the process is similar to the late stage of ribbon-induced transition (Nishioka, Asai & Iida 1981). The bypass transition required a threshold amplitude for the eddies. For the purpose of further clarification of this fact in the pipe flow, an additional single-peak experiment was carried out at lower input amplitude. A high-shear layer was formed that signified the existence of a hairpin vortex, but transition did not occur and the disturbances decayed farther downstream (the observation corresponds to the intermediate regime reported by ETW). Thus, the result demonstrates the need for a threshold amplitude in the pipe flow as well.

Hairpin vortices in a boundary layer were investigated experimentally by Acarlar & Smith (1987*a, b*) and Haidari & Smith (1994). The hairpin vortices were generated by a hemispheric protuberance and the injection of fluid into the boundary layer. The results indicated the need for a threshold level of the disturbance amplitude and Reynolds number to trigger the regeneration of hairpin vortices. One may speculate that a hairpin vortex is a common element in both regular and in bypass routes to transition. There may be, therefore, a more general criterion for the transition to turbulence than is known today. Such a criterion must be related to dynamics of hairpin vortices in a shear flow (it is pertinent to mention here the recent results by Levinski & Cohen 1995).

The present experiment is concerned with a transition triggered by wave trains induced through the pipe wall. It would also be interesting to link the current observations of the hairpin vortices to the dynamics of the ‘natural conditions’. Wygnanski & Champagne (1973) observed that for smooth inlets, transition occurs as a result of instabilities in the boundary layer long before the flow becomes fully developed in the pipe. This type of transition gives rise to turbulent slugs that occupy the entire cross-section of the pipe. When a large disturbance was introduced into the inlet, a mixed laminar and turbulent flow was observed far downstream for $2000 < Re < 2700$. This type of turbulent-like flow was called a ‘puff’. Our experiments were carried out in the same Reynolds number range, and one can expect that the dynamics of puffs may be somehow interpreted in terms of the dynamics of hairpin vortices. Shan *et al.* (1999) investigated numerically a puff and a slug that were triggered by a disturbance in the form of local blowing and suction of fluid through a slot in the pipe wall. They found streamwise vortices in the trailing-edge region. The results indicate that there might be a link to the present experiments using the wave trains inasmuch as the transition is also accompanied by streamwise vortices.

The authors gratefully acknowledge fruitful discussions of the results with Professor Y. Kachanov, who made many useful recommendations regarding the experiment and the analysis of the results. We also would like to thank Professor D. Rempfer and Dr J. Reuter for their helpful discussion of the results and for analysis of the data by using DNS. We also thank Dr R. Bowles for letting us see his review on the physical mechanisms of boundary-layer transition. We have also benefited from useful comments by Professor F. T. M. Nieuwstadt and by an anonymous referee’s comments on the first draft of this paper. The work was supported by the Israel Science Foundation.

REFERENCES

- ACARLAR, M. S. & SMITH, C. R. 1987*a* A study of hairpin vortices in a laminar boundary layer. Part 1. Hairpin vortices generated by a hemisphere protuberance. *J. Fluid Mech.* **175**, 1–41.
- ACARLAR, M. S. & SMITH, C. R. 1987*b* A study of hairpin vortices in a laminar boundary layer. Part 2. Hairpin vortices generated by fluid injection. *J. Fluid Mech.* **175**, 43–83.
- ASAI, M. & NISHIOKA, M. 1995 Boundary-layer transition triggered by hairpin eddies at subcritical Reynolds numbers. *J. Fluid Mech.* **297**, 101–122.
- ASAI, M. & NISHIOKA, M. 1997 Development of wall turbulence structure in transitional flows. In *Theoretical and Applied Mechanics 1996, 19th IUTAM Congress, 1996 Kyoto, Japan*. (ed. T. Tatsumi, E. Watanabe & T. Kambe), pp. 121–138. Elsevier.
- ASAI, M., SAWADA, K. & NISHIOKA, M. 1996 Development of turbulent patch in a subcritical boundary-layer transition. *Fluid Dyn. Res.* **18**, 151–164.
- BAGGETT, J. S. & TREFETHEN, L. N. 1997 Low-dimensional models of subcritical transition to turbulence. *Phys. Fluids* **9**, 1043–1053.
- BAKE, S., KACHANOV, Y. S. & FERNHOLZ, H. H. 1996 Subharmonic K-regime of boundary layer breakdown. In *Transitional Boundary Layers in Aeronautics*. pp. 81–88. North.
- BERGSTRÖM, L. 1992 Initial algebraic growth of small disturbances in pipe Poiseuille flow. *Stud. Appl. Maths* **87**, 61–79.
- BERGSTRÖM, L. 1993 Optimal growth of small disturbances in pipe Poiseuille flow. *Phys. Fluids A* **5**, 2170–2720.
- BERGSTRÖM, L. 1999 Self-sustained amplification of disturbances in pipe Poiseuille flow. *Eur. J. Mech. B/Fluids* **18**, 635–647.
- BERLIN, S., LUNDBLADH, A. & HENNINGSON, D. 1994 Spatial simulation of oblique transition in a boundary layer. *Phys. Fluids* **6**, 1949–1951.
- BERLIN, S., WIEGEL, M. & HENNINGSON, D. S. 1999 Numerical and experimental investigations of oblique boundary layer transition. *J. Fluid Mech.* **393**, 23–57.
- BOBERG, L. & BROSA, U. 1988 Onset of turbulence in a pipe. *Z. Naturforsch. A* **43a**, 697–726.
- BORODULIN, V. I. & KACHANOV, Y. S. 1988 Role of the mechanism of local secondary instability in the K-breakdown of a boundary layer. *Izv. Sib. Otd. Akad. Nauk SSSR, Tekh. Nauk.* No. 5, 65–77 (in Russian).
- BORODULIN, V. I. & KACHANOV, Y. S. 1995 Formation and development of coherent structures in a transitional boundary layer. *J. Appl. Mech. Tech. Phys.* **36**, 532–564 (transl. from Russian).
- BORODULIN, V. I., GAPONENKO, V. R., KACHANOV, Y. S., LEE, C. B., LIAN, Q. X. & DU, X. D. 1998 Investigation of mechanisms of development and breakdown of coherent structures in transitional boundary layer. In *Laminar-Turbulent Transition Mechanisms and Prediction. EUROMECH Colloquium 380, Gottingen, Book of abstracts*, Abstract No. 1.
- BOWLES, R. I. 2000 Transition to turbulent flow in aerodynamics. *Phil. Trans. R. Soc. A* **358**, 245–260.
- BUTLER, K. M. & FARREL, B. F. 1992 Three-dimensional optimal perturbations in viscous shear flow. *Phys. Fluids A* **4**, 1637–1650.
- DARBYSHIRE, A. G. & MULLIN, T. 1995 Transition to turbulence in constant-mass-flux pipe flow. *J. Fluid Mech.* **289**, 83–114.
- DRAAD, A. A., KUIKEN, G. & NIEUWSTADT, F. T. M. 1998 Laminar-turbulent transition in pipe flow for Newtonian and non-Newtonian fluids. *J. Fluid Mech.* **377**, 267–312.
- ELIAHOU, S., HAN, G., TUMIN, A. & WYGNANSKI, I. 1998*a* Laminar-turbulent transition in pipe Poiseuille flow and its similarity to transition in boundary layers. *NASA/CP-1998-206958*, pp. 353–365.
- ELIAHOU, S., TUMIN, A. & WYGNANSKI, I. 1998*b* Laminar-turbulent transition in Poiseuille pipe flow subjected to periodic perturbation emanating from the wall. *J. Fluid Mech.* **361**, 333–349 (referred to here in as ETW).
- ELLINGSON, T. & PALM, E. 1975 Stability of linear flow. *Phys. Fluids* **18**, 487–488.
- ELOFSSON, P. A. 1998 An experimental study of oblique transition in a Blasius boundary layer flow. *TRITA-MEK, Tech. Rep. 4*, Dept. of Mechanics, KTH, Stockholm, Sweden.
- ELOFSSON, P. A. & ALFREDSSON, P. H. 1998 An experimental study of oblique transition in plane Poiseuille flow. *J. Fluid Mech.* **358**, 177–202.
- FOX, J. A., LESSEN, M. & BHAT, W. V. 1968 Experimental investigation of the stability of Hagen-Poiseuille flow. *Phys. Fluids* **11**, 1–4.

- GAPONENKO, V. R. & KACHANOV, Y. S. 1994 New method of generation of controlled spectrum instability waves in the boundary layer. *7th Intl Conf. on Methods of Aerophysical Research, Proc. Part 1*. pp. 90–97. Inst. Theoret. Appl. Mech., Novosibirsk.
- GUSTAVSSON, L. H. 1991 Energy growth of three-dimensional disturbances in plane Poiseuille flow. *J. Fluid Mech.* **224**, 242–260.
- Haidari, A. H. & Smith, C. R. 1994 The generation and regeneration of single hairpin vortex. *J. Fluid Mech.* **277**, 135–162.
- HAMA, F. R., LONG, J. D. & HEGARTY, J. C. 1957 On transition from laminar to turbulent flow. *J. Appl. Phys.* **28**, 388–394.
- HAMA, F. R. & NUTANT, J. 1963 Detailed flow-field observations in the transition process in a thick boundary layer. *Proc. 1963 Heat Transfer & Fluid Mech. Inst. Pal Alto, CA*, pp. 388–394. Stanford University Press.
- HULTGREN, L. S. & GUSTAVSSON, L. H. 1981 Algebraic growth of disturbances in a laminar boundary layer *Phys. Fluids* **24**, 1000–1004.
- JOSLIN, R. D., STREET, C. L. & CHANG, C. L. 1992 Oblique wave breakdown in incompressible boundary layer computed by spatial DNS and PSE theory. In *Instability, Transition and Turbulence* (ed. M. Y. Hussaini, A. Kumar & C. L. Street), pp. 304–310. Springer.
- KACHANOV, Y. S. 1994 Physical mechanisms of laminar-boundary-layer transition. *Ann. Rev. Fluid Mech.* **26**, 411–482.
- KACHANOV, Y. S., KOZLOV, V. V. & LEVCHENKO, V. Y. 1977 Nonlinear development of a wave in a boundary layer. *Fluid Dyn.* **12**, 383–390 (transl. from Russian).
- KACHANOV, Y. S., KOZLOV, V. V., LEVCHENKO, V. Y. & RAMAZANOV, M. P. 1984 Experimental study of K-regime breakdown of laminar boundary layer. *Preprint No. 9–84. Inst. Theoret. Appl. Mech., Siberian Div. USSR Acad. Sci., Novosibirsk* (in Russian).
- KACHANOV, Y. S., KOZLOV, V. V., LEVCHENKO, V. Y. & RAMAZANOV, M. P. 1985 Experimental study of K-regime breakdown of laminar boundary layer. *Laminar-Turbulent Transition, IUTAM Symposium, 1984 Novosibirsk, USSR* (ed. V. Kozlov). Springer.
- KACHANOV, Y. S., KOZLOV, V. V., LEVCHENKO, V. Y. & RAMAZANOV, M. P. 1989 On the nature of K-breakdown of a laminar boundary layer. *Izv. Sib. Otd. Akad. Nauk SSSR, Tekh. Nauk.* No. 2, 124–158 (in Russian).
- KASKEL, A. 1961 Experimental study of the stability of pipe flow II. Development of disturbance generator. *Jet Propulsion Laboratory Tech. Rep.* 32–138.
- KLEBANOFF, P. S., TIDSTROM, K. D. & SARGENT, L. M. 1962 The three-dimensional nature of boundary layer instability. *J. Fluid Mech.* **12**, 1–34.
- KLEISER, L. & ZANG, A. 1991 Numerical simulation of transition in wall-bounded shear flows. *Ann. Rev. Fluid Mech.* **23**, 495–537.
- KOVASZNAV, L. S. G., KIBENS, V. & BLACKWELDER, R. F. 1970 Large-scale motion in the intermittent region of a turbulent boundary layer. *J. Fluid Mech.* **41**, 283–325.
- KOVASZNAV, L. S., KOMODA, H. & VASUDEVA, B. R. 1962 Detailed flowfield transition, *Proc. 1962 Heat Transfer & Fluid Mech. Inst. Pal Alto, CA*, pp. 1–26. Stanford University Press.
- LANDAHL, M. T. 1980 A note on an algebraic instability of inviscid parallel shear flows. *J. Fluid Mech.* **98**, 243–251.
- LEITE, R. J. 1959 An experimental investigation of the stability of Poiseuille flow. *J. Fluid Mech.* **5**, 81–97.
- LEVINSKI, V. & COHEN, J. 1995 The evolution of a localized vortex disturbance in external flows. Part 1. Theoretical considerations and preliminary experimental results. *J. Fluid Mech.* **289**, 159–177.
- MA, B., DOORNE, C. W. H. VAN, ZANG, Z. & NIEUWSTADT, F. T. M. 1999 On the spatial evolution of wall-imposed periodic disturbance in pipe Poiseuille flow at a $Re = 3000$. Part 1. Subcritical disturbance. *J. Fluid Mech.* **398**, 181–224.
- MAYER, E. W. & RESHOTKO, E. 1997 Evidence for transient disturbance growth in a 1961 pipe-flow experiment. *Phys. Fluids* **9**, 242–244.
- MORKOVIN, M. V. 1993 Bypass-transition research: issues and philosophy. In *Instabilities and Turbulence in Engineering Flows* (ed. D. E. Ashpis, T. B. Gatski & R. Hirsh), pp. 3–30. Kluwer.
- MORKOVIN, M. V. & RESHOTKO, E. 1990 Dialogue on progress and issues in stability and transition research. In *Laminar-Turbulent Transition, IUTAM Symposium, 1989 Toulouse, France* (ed. D. Arnal & R. Michel), pp. 3–29. Springer.

- NISHIOKA, M. & ASAI, M. 1985 Some observations of the subcritical transition in plane Poiseuille flow. *J. Fluid Mech.* **150**, 441–450.
- NISHIOKA, M., ASAI, M. & IIDA, S. 1981 Wall phenomena in the final stage of transition to turbulence. In *Transition and turbulence, Proc. of Symposium at the University of Wisconsin–Madison, 1980* (ed. R. E. Meyer). Academic.
- O’SULLIVAN, P. L. & BREUER, K.S. 1994 Transient growth in circular pipe flow. I. Linear disturbances. *Phys. Fluids* **6**, 3643–3651.
- REDDY, S. C. & HENNINGSON, D. S. 1993 Energy growth in viscous channel flows. *J. Fluid Mech.* **252**, 209–238.
- REDDY, S. C., SCHMID, P. J., BAGGET, J. S. & HENNINGSON, D. S. 1998 On stability of streamwise streaks and transition thresholds in plane channel flows. *J. Fluid Mech.* **365**, 269–303.
- RESHOTKO, E. 1994 Boundary layer instability, transition and control. *AIAA Paper* 94-0001.
- RESHOTKO, E. & TUMIN, A. 1999 Spatial theory of transient growth in a circular pipe flow. *Bull. Am. Phys. Soc.* **44**, 72.
- REUTER, J. & REMPFER, D. 1998 Direct numerical simulation of spatial pipe flow transition using a hybrid spectral/finite-difference scheme. *Bull. Am. Phys. Soc.* **43**, 2106–2107.
- REUTER, J. & REMPFER, D. 2000 A hybrid spectral/finite-difference scheme for the simulation of pipe-flow transition. In *Laminar–Turbulent Transition, IUTAM Symposium, 1999 Sedona, USA* (ed. H. Fasel & W. Saric). Springer.
- RIST, U. & FASEL, H. 1995 Direct numerical simulation of controlled transition in a flat-plate boundary layer. *J. Fluid Mech.* **298**, 211–248.
- RIST, U. & KACHANOV, Y. S. 1995 Numerical and experimental investigation of the K-regime of boundary-layer transition. In *Laminar–Turbulent Transition, IUTAM Symposium, 1994 Sendai, Japan* (ed. R. Kobayashi). Springer.
- RUBIN, Y., WYGNANSKI, I. & HARITONIDIS, J. H. 1980 Further observation on transition in a pipe. In *Laminar–Turbulent Transition, IUTAM Symposium, 1979 Stuttgart, Germany* (ed. R. Eppler & H. Fasel), pp. 19–26. Springer.
- SCHMID, P. J. & HENNINGSON, D. S. 1992 Channel flow transition induced by a pair of oblique waves. In *Instability, Transition and Turbulence* (ed. M. Y. Hussaini, A. Kumar & C. L. Street), pp. 356–366. Springer.
- SCHMID, P. J. & HENNINGSON, D. S. 1994 Optimal energy density growth in Hagen–Poiseuille flow. *J. Fluid Mech.* **277**, 197–225.
- SHAN, H., MA, B., ZHANG, Z. & NIEUWSTADT, F. T. M. 1999 Direct numerical simulation of a puff and slug in transitional cylindrical pipe flow. *J. Fluid Mech.* **387**, 39–60.
- TREFETHEN, L. N., TREFETHEN, A. E., REDDY, S. C. & DRISCOLL, T. A. 1993 Hydrodynamic stability without eigenvalues. *Science* **261**, 578–584.
- TREFETHEN, A. E., TREFETHEN, L. N. & SCHMID, P. J. 1999 Spectra and pseudospectra for pipe Poiseuille flow. *Computer Methods in Applied Mechanics and Engineering* **175**, 413–420.
- WALEFFE, F. 1997 On a self-sustaining process in shear flows. *Phys. Fluids* **9**, 883–900.
- WILLIAMS, D. R., FASEL, H. & HAMA, F. R. 1984 Experimental determination of the three-dimensional vorticity field in the boundary-layer transition process. *J. Fluid Mech.* **149**, 179–203.
- WYGNANSKI, I. J. & CHAMPAGNE, F. H. 1973 On transition in a pipe. Part 1. The origin of puffs and slugs and the flow in a turbulent slug. *J. Fluid Mech.* **59**, 281–335.